

## Static and Dynamic Quenching of Protein Fluorescence. I. Bovine Serum Albumin

ISAAC FELDMAN,\* DOLORES YOUNG,† and ROBERT McGUIRE,††

*Department of Radiation Biology and Biophysics, School of Medicine and Dentistry, University of Rochester, Rochester, New York 14642*

### Synopsis

The fluorescence parameters, lifetime, relative quantum yield, maximum and mean wavelength, half-width, and polarization, of bovine serum albumin (BSA) were measured at 15°C in aqueous solutions containing varying concentrations of different chemical perturbants, glycerol,  $\text{Cu}^{2+}$  ions, guanidine hydrochloride, and urea. By considering a quenching mechanism as being either dynamic or static, depending upon whether the quenching is or is not accompanied by a change in the fluorescence lifetime, we were able to correlate the changes produced in the various fluorescence parameters by the different chemical perturbants with changes in macromolecular structure as the concentration of perturbant was gradually increased. The addition of glycerol and of  $\text{Cu}^{2+}$  ions indicated that in aqueous BSA both tryptophan residues are below the surface of the macromolecule, out of contact with solvent water, and, as a consequence, they are statically quenched. "Ultra-Pure" guanidine hydrochloride at 2.4 *M* or more caused a drastic conformation change, which resulted in the emergence of a visible tyrosine peak at 304 nm in the BSA fluorescence spectrum when either 260- or 270-nm excitation was employed. With the same excitation, the enhancement of BSA tyrosine fluorescence by 6-8 *M* ultra-pure urea produced only a shoulder near 304 nm in the BSA fluorescence spectrum. We have introduced the use of a new relative quantum yield for protein fluorescence,  $q'$ , referenced to the quantum yield of unquenched free tryptophan, which eliminates the quenching action of water from the reference.

### INTRODUCTION

It is well known that the intrinsic fluorescence of proteins emanates from tyrosine and tryptophan residues<sup>1</sup> and that it supplies a very sensitive means of studying internal protein structure and changes therein.<sup>2</sup> Its use, however, has been almost entirely empirical, because the wide variation in the microenvironment of protein fluorophores makes theoretical analysis almost prohibitively complex. Cowgill<sup>3</sup> has classified fluorescent protein tryptophan and tyrosine residues in terms of their exposure to aqueous solvent and to the various known quenching agents inherent in a protein, e.g., peptide carbonyl, disulfide, phenolate, and carboxyl groups.

\* To whom reprint requests should be addressed.

† Present Address: Biology Dept., Syracuse University, Syracuse, N.Y.

†† Present Address: Biochemistry Dept., University of Massachusetts Medical School, Worcester, Mass.

More recently, Burstein et al.<sup>4</sup> put forth a model for the distribution of the fluorescent tryptophan residues in proteins based on three discrete spectral classes: I—buried in nonpolar regions with emission  $\lambda_{\max} = 330\text{--}332\text{ nm}$ ; II—on the surface but in limited contact with solvent water, which is probably immobilized by bonding at the macromolecular surface, with  $\lambda_{\max} = 340\text{--}342\text{ nm}$ ; and III—completely exposed to water, with emission  $\lambda_{\max} = 350\text{--}352\text{ nm}$ .

Our own investigation of the fluorescence of bovine serum albumin (BSA) gave results that contradict the model of Burstein et al. We have studied the effect of several chemical perturbants (glycerol,  $\text{Cu}^{2+}$  ions, urea, and guanidine hydrochloride) on the fluorescence properties (quantum yield, lifetime, polarization, spectral positions, and half-width) of BSA, which is one of the 27 proteins studied by Burstein et al. By assuming additivity and mutual independence for the spectral contributions of their three classes of fluorescent tryptophan residues, these authors calculated that in BSA *all* of the tryptophan fluorescence issues from surface residues, 80% from those in Class II, and 20% from those in Class III. (The fractional nature of their calculated numbers of fluorescent residues in each class was considered by Burstein et al. as an indication of the existence of a mixture of molecules differing in conformation.) In contrast, our results indicate that in aqueous BSA most of the fluorescence is emitted from residues situated below the surface, despite the fact that  $\lambda_{\max}$  is relatively high, 345 nm.

Our work also shows that simple considerations of the relative importance of dynamic and static quenching processes in a protein under various conditions, such as solvent perturbation and denaturation, can furnish considerable information concerning the macromolecular structure. As in our previous paper,<sup>5</sup> we will employ the terms "dynamic" and "static" to denote whether a quenching process does, or does not, involve a change in the fluorescence lifetime. Thus, collisional quenching,<sup>6</sup> resonance transfer,<sup>7</sup> and the formation of a nonfluorescent excited-state complex with a lifetime *shorter* than the fluorescence lifetime of the uncomplexed fluorescent species<sup>6</sup> are dynamic processes, but static quenching follows from the formation of a nonfluorescent ground-state complex or of a nonfluorescent excited-state complex with a lifetime *greater* than the fluorescence lifetime.<sup>6,8,9</sup> (We consider the fluorescer-quencher pair concept of Boaz and Rollefson,<sup>8</sup> who coined the term "static quenching," to be included in our use of the term "nonfluorescent ground-state complex.")

## EXPERIMENTAL

### Materials

The BSA used was Calbiochem grade A. Application of the analytical method of Ettinger et al.<sup>10</sup> showed that only a negligible amount of citrate,  $<0.005\text{ mol/mol}$  BSA, was present.

A specially selected solution of colloidal silica (IBD-1019-69), a gift from E. I. du Pont de Nemours and Co, was used as the reference scattering solution in lifetime measurements and in periodically checking the intensity calibration of the spectrofluorimeter Xenon lamp source.

Ultra-pure urea and ultra-pure guanidine hydrochloride (GuHCl) were purchased from Mann Research Laboratories. The absorbance at 260 nm, the wavelength used for most of our work, was 0.055 for 8 *M* urea and 0.043 for 6.4 *M* guanidine hydrochloride, when a 1-cm cell was used.

Glycerol, which was sufficiently pure for very accurate fluorescence work, was prepared by very slow filtration of a suspension of Mallinkrodt reagent grade glycerol and prewashed-predried Fisher Norit A charcoal through prerinsed-predried Millipore paper under a pressure of  $\sim 24$  in Hg. The filtrate was collected after its absorbance became  $< 0.010$ .

Solutions were prepared with water, which had been redistilled in an all-glass still, and which had been monitored with the aid of the spectrofluorimeter for negligible light scattering.

### Fluorescence Lifetime, Spectra, and Intensity Measurements

Fluorescence lifetime, spectra, and intensity measurements were as described in our previous paper.<sup>5</sup>

Fluorescence lifetimes were measured at 15°C with a TRW nanosecond spectral source to a reproducibility of  $\pm 0.1$  nsec, although the accuracy was probably  $\sim 10\%$ . A 270-nm interference filter (Optics Technology) was placed in the excitation path, and a 7-51 filter (Corning 5970) was used in the emission path. About 90% of the light transmitted through the latter filter has a wavelength above 330 nm. About 90% of any tyrosine emission occurs below this wavelength, and thus is eliminated from measurement. About 90% of tryptophan fluorescence occurs above 330 nm, so that with this filter arrangement it is primarily the lifetime of the tryptophan fluorescence of the protein that is measured.

Corrected fluorescence emission spectra were obtained at 15°C with 260-nm excitation using a completely automated spectrofluorimeter, consisting of an Aminco-Kiers spectrofluorimeter linked to a PDP7 digital computer. The computer was programmed to print out the integrated area (intensity) under the fluorescence curve, the maximum and mean wavelengths ( $\lambda_{\max}$  and  $\lambda_{\text{mean}}$ ) of a spectral band, and the half-width ( $\Delta\lambda_{1/2}$ ). The computer also was programmed to analyze the fluorescence spectrum for the existence of more than one Cauchy (Lorentz) component<sup>11</sup> and, when two spectral components were indicated, to print out the  $\lambda_{\text{mean}}$  and fluorescence intensity of each component corresponding to assumed  $\lambda_{\max}$  values for the components. Additivity of the intensities of spectral components was assumed.

In each case the fluorescence spectrum and the lifetime were obtained with the same solution in the same cuvette.

A Beckman DU spectrophotometer was employed for absorbance measurements.

### Polarization of Fluorescence

For polarization measurements an Aminco polarizer accessory was used in conjunction with our computerized spectrofluorimeter. It consists of two Glan-Thompson polarizer prisms, each rotatable through a 90° angle, mounted on the cell holder to permit passage of radiation in either of two directions perpendicular to the direction of propagation of the incident light. Assuming that incident light is propagated in the  $X$  direction and that the fluorescence is observed in the  $Y$  direction, the orientation of either polarizer is designated either  $E$  or  $B$ , depending upon whether it passes only light polarized with its electric vector in the  $Z$  direction or the  $Y$  direction, respectively.

The degree of polarization  $P$  is defined as:

$$P = (I_{||} - I_{\perp}) / (I_{||} + I_{\perp}) \quad (1)$$

where  $I_{||}$  and  $I_{\perp}$  refer to the intensities of the components of the emitted light beam resolved in directions polarized parallel and perpendicular to the polarization vector of the polarized incident excitation. When the Aminco polarizer accessory is employed, Eq. (1) is equivalent to<sup>12</sup>

$$P_p = (I_{EE} - TI_{EB}) / (I_{EE} + TI_{EB}) \quad (2)$$

when linearly polarized incident light is employed. The first subscript denotes the orientation of the polarizer in the exciting light path, while the second subscript denotes the orientation of the polarizer in the emission path.  $T$  is the transmission coefficient  $I_{BE}/I_{BB}$ , which corrects for the fact that the efficiencies of the monochromator and photomultiplier are different for light polarized in different directions.

Equation (2) becomes:

$$P_n = (I_{nB} - TI_{nB}) / (I_{nE} + TI_{nB}) \quad (3)$$

when there is no polarizer in the incident light path, i.e., when natural exciting light is being used.

Perrin<sup>13</sup> has shown that  $P_p$  and  $P_n$  are related by the equation:

$$P_p = 2P_n / (1 + P_n) \quad (4)$$

when  $P_n$  is measured with *completely* unpolarized incident light.

For our paper most of the  $P$  measurements were made using linearly polarized incident light, but with solutions of very low fluorescence intensity it was necessary to use natural incident light. In the latter case, for the sake of consistent presentation of results, the observed  $P_n$  values were converted to  $P_p$  values by Eq. (4). Thus, all of our reported  $P$  values are  $P_p$ . The validity of Eq. (4) for our equipment was verified with several solutions of higher concentration. This also demonstrated that polarization of the exciting light source did not contribute significant error.

Since the  $T$  value in Eqs. (3) and (4) is dependent on the wavelength of the emission, it was determined at 2-nm intervals from 302 to 430 nm. A simple relationship,  $T = 1.9864 - 0.00180\lambda$ , was found.

The polarizers cause a spectral shift.<sup>12</sup> With excitation and emission spectra of 45 solutions, containing either tyrosine, tryptophan, or BSA, we observed a 4-nm increase in  $\lambda_{\max}$  when the polarizer located in the same light path as the *variable* monochromator was reoriented from the *E* to the *B* orientation. This spectral shift correction was applied *prior* to calculating the polarization.

The computer was programmed to calculate the *P* values automatically from the spectra using either Eq. (3) or (4).

### Quantum Yield $q'$

Because of the considerable disagreement concerning the correct values for the absolute quantum yield of tyrosine and tryptophan, even among distinguished authors<sup>14,15</sup> of reviews in the same monograph, protein quantum yields are generally obtained as relative values, usually with aqueous tyrosine or aqueous tryptophan as the reference substance, and changes produced in these relative values are interpreted in terms of changes in protein structure.<sup>16</sup> As we have shown previously,<sup>5</sup> water quenches the fluorescence of both of these amino acids by a dynamic process, but it quenches tryptophan fluorescence so much more strongly than tyrosine fluorescence that it actually reverses their natural order.

We believe that it is more enlightening, when relative values are used, to compare the protein quantum yield with an unquenched standard, which will make the amount of quenching of protein fluorescence more readily apparent. For class B proteins,<sup>17</sup> such as BSA, whose fluorescence is mainly that of the tryptophan content, tryptophan should be a preferable standard, while tyrosine would be preferable for class A proteins,<sup>17</sup> which contain no tryptophan. We showed earlier<sup>5</sup> that neither tyrosine nor tryptophan, in their free state, are quenched significantly by glycerol. Hence, in this paper we have employed a newly defined relative quantum yield  $q'$ , which is the quantum yield of the protein divided by the quantum yield of unquenched tryptophan (i.e., of 0.01 mM tryptophan in glycerol), i.e.,  $q'_x = (F_x/A_x) \div (F_{\text{try,G}}/A_{\text{try,G}})$ , where *F* is the fluorescence intensity and *A* is the absorbance of the sample and of the glycerol solution of tryptophan represented, respectively, by the subscripts *x* and try,G.

For this work  $q'$  (i.e.,  $q'_x$ ) was obtained as the ratio  $q_x/q_{\text{try,G}}$  where the *q* values are the conventional relative quantum yields for *x* and try,G with aqueous 0.05 mM tyrosine as the standard. The  $q_{\text{try,G}}$  value, i.e., in pure glycerol, was obtained by extrapolation of the linear plot obtained earlier<sup>5</sup> for the glycerol concentration dependence of the *q* of 0.01 mM tryptophan in glycerol-water mixtures ranging from 0 to 90% glycerol. The quantum yield value for the aqueous standard cancels out. Measurement of the absolute quantum yield of tryptophan in glycerol would be subject to the same uncertainty as presently exists for the aqueous tryptophan absolute value, so that only a relative value, such as  $q'$ , seems practical at present.

## RESULTS

Figure 1 shows the dependence upon glycerol concentration of various fluorescence parameters of 0.02% BSA in glycerol–water mixtures of varying composition at 15°C. 260-nm excitation was employed for the spectral parameters  $q'$ ,  $\lambda_{\max}$ , and  $\Delta\lambda_{1/2}$ , while for  $\tau$  the filter arrangement described above was used. The  $\tau$  and  $q'$  plots are in Figure 1a, while the  $\lambda_{\max}$  and  $\Delta\lambda_{1/2}$  plots are in Figure 1b.

The values for the polarization  $P_p$  of the fluorescence for these same solutions of BSA in glycerol–water mixtures are presented in Figure 2 as reciprocal values  $P^{-1}$  plotted against the  $\tau/\eta$  ratio,  $\eta$  being the solvent viscosity. We did not employ the customary Perrin plot, which has  $T/\eta$  as the abscissa, because in these solutions, even though  $T$  was kept constant, there was a variation in  $\tau$  [Figure 1a and Eq. (5)]. The polarization of fluorescence was constant within an uncertainty of  $\pm 0.01$  over the emission range 330–380 nm, where any contribution of tyrosine fluorescence is negligible

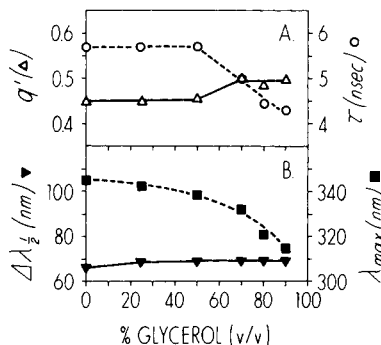


Fig. 1. Variation of fluorescence parameters of 0.02% BSA in glycerol–water mixtures of varying composition at 15°C. Spectral parameters,  $q'$ ,  $\lambda_{\max}$ , and  $\Delta\lambda_{1/2}$ , were obtained with 260-nm excitation. Filters, described in text, were employed in the  $\tau$  measurements.

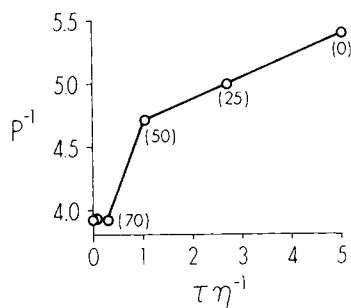


Fig. 2. Dependence of reciprocal of the polarization of the fluorescence of 0.02% BSA upon fluorescence lifetime and viscosity in glycerol–water mixtures of varying composition at 15°C with linearly polarized 260-nm excitation.  $P$  values are averages over the 330–380-nm emission range. Numbers on graph indicate % glycerol.

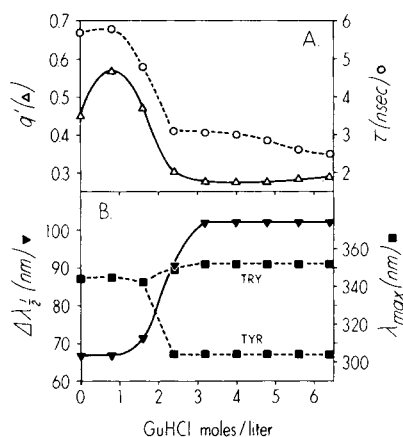


Fig. 3. Variation of fluorescence parameters of 0.02% BSA in aqueous solutions of guanidine hydrochloride of varying concentration at 15°C. Splitting of  $\lambda_{\max}$  plot indicates presence of two emission peaks.

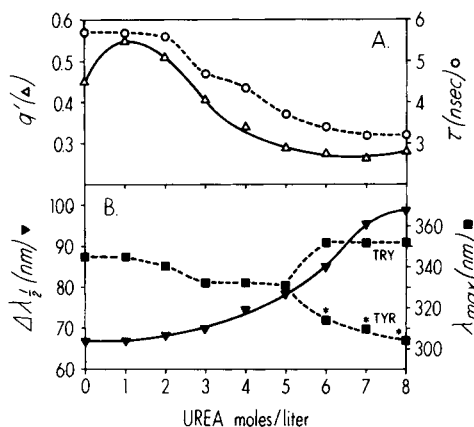


Fig. 4. Variation of fluorescence parameters of 0.02% BSA in aqueous solutions of urea of varying concentration at 15°C. Starred points indicate presence of a conspicuous shoulder.

even for 260-nm excitation. The  $P$  values presented in Figure 2 are the average values observed over this wavelength range. The viscosity values for the glycerol-water mixtures at 15°C used as the abscissas in Figure 2 were obtained by extrapolating  $\log \eta$  versus  $T^{-1}$  plots of the 20°, 25°, and 30°C literature values<sup>18</sup> of  $\eta$  at the various solvent compositions of interest. These plots are linear for all glycerol-water (wt %) compositions between 0 and 100% glycerol.

In Figure 3 are presented curves showing the effect of the fluorescence parameters,  $\tau$ ,  $q'$ ,  $\Delta\lambda_{1/2}$ , and  $\lambda_{\max}$ , produced by gradually adding GuHCl up to 6.4  $M$  at 15°C. Figure 4 is a similar graph for urea concentrations up to 8  $M$ . Excitation energy was the same as for Figure 1.

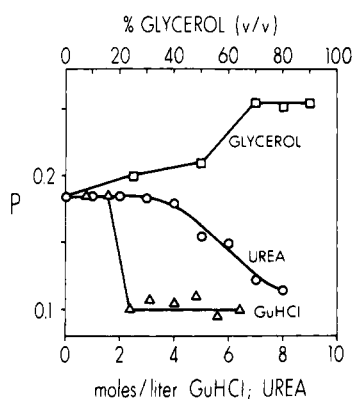


Fig. 5. Variation of polarization of the fluorescence of 0.02% BSA produced by chemical perturbants, GuHCl, urea, and glycerol, at varying concentration at 15°C with linearly polarized 260-nm excitation.

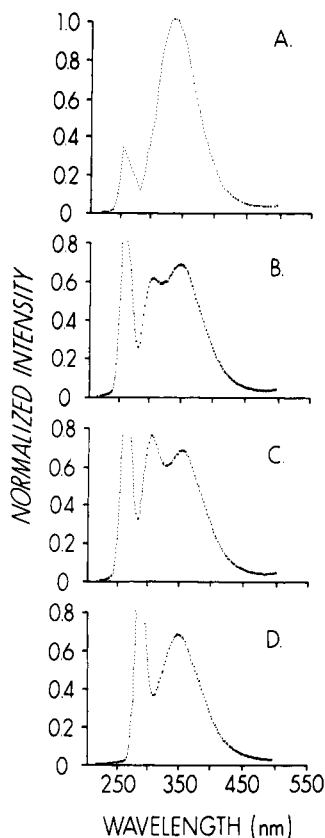


Fig. 6. Fluorescence spectra of 0.02% BSA in various concentrations of aqueous GuHCl at 15°C. (A), (B) and (C) GuHCl concentrations—0.8, 2.4, and 6.4 *M*; 260-nm excitation. (D) GuHCl concentration—6.4 *M*; 290-nm excitation. Note absence of 304-nm tyrosine peak in (A) and (D). The peaks on extreme left are Rayleigh scatter peaks.



The polarization values of the BSA fluorescence in these GuHCl and urea solutions are given in Figure 5. As in Figure 2, these  $P$  values are the averages over the 330–380-nm emission range, so that, despite the fact that some tyrosine fluorescence is obvious (Figure 6) with  $[\text{GuHCl}] \geq 2.4\text{ M}$  and with  $[\text{urea}] \geq 6\text{ M}$ , these  $P$  values are primarily for tryptophan fluorescence. For comparison, the polarization curve for BSA in glycerol–water mixtures (same data as in Figure 2) is also included in Figure 5.

Figure 6 shows the fluorescence spectrum of BSA for 260-nm excitation at 15°C when different GuHCl concentrations are present. It clearly demonstrates the appearance of a tyrosine peak when  $[\text{GuHCl}] = 2.4\text{ M}$  and its increasing intensity as  $[\text{GuHCl}]$  was further increased up to 6.4 M.

## DISCUSSION

It is universally accepted that most of the fluorescence of aqueous tryptophan-containing proteins emanates from the tryptophan residues, but that structural changes, such as those caused by denaturation, may cause the appearance of a significant amount of tyrosine fluorescence also. Nevertheless, as we explained above, our  $\tau$  and  $P$  values refer primarily to the tryptophan contribution, even when the tyrosine fluorescence is significantly large.

The  $q'$ ,  $\Delta\lambda_{1/2}$ , and  $\lambda_{\text{max}}$  values result from statistical averages of both the tryptophan and the tyrosine emissions, where both types do occur, since we employed 260-nm excitation and the entire emission spectrum is involved in these measurements. However, our interpretations of these parameters are based entirely on the observed *changes* in their magnitudes, with the starting points being the aqueous BSA values to which the tyrosine contributions are experimentally insignificant. Weber's use<sup>19</sup> of difference fluorescence spectra and his matrix method of analysis<sup>20</sup> did suggest that tyrosine does contribute a small amount to the fluorescence of aqueous BSA when 280-nm excitation is employed. However, as pointed out by Konev,<sup>21</sup> Weber seems to have ignored energy transfer from tyrosine to tryptophan, which, Longworth<sup>22</sup> asserts, amounts to  $\sim 20\%$  of the energy absorbed at 280 nm.

One can, in fact, employ a simple geometric procedure to demonstrate that any significant tyrosine contribution (e.g., 5%) to the total fluorescence of BSA can be detected by a measurable increase in  $\Delta\lambda_{1/2}$ . Using the half-widths of aqueous tyrosine and tryptophan, 33 and 69 nm, respectively, and the  $\lambda_{\text{max}}$  values, 304 and 345 nm, of aqueous tyrosine and aqueous BSA, respectively, one can superimpose upon the BSA spectrum a small isosceles triangle to represent a small tyrosine contribution, e.g., with half-width equal to 33 nm and height equal to 10% (i.e.,  $5\% \times 69/33$ ) of the peak intensity of the BSA spectrum, when a 5% tyrosine contribution is considered. Assuming additivity of the tyrosine and tryptophan contributions in the region of overlap of the BSA spectrum and the simulated tyrosine spectrum, one can construct the new spectrum, i.e., with 5% tyrosine contribution, which has a 4-nm larger  $\Delta\lambda_{1/2}$  value than the original

BSA spectrum. Such a calculation becomes less accurate for larger tyrosine contributions, which cannot be accurately represented by isosceles triangles, but the continual increase in  $\Delta\lambda_{1/2}$  as the tyrosine contribution increases can be demonstrated.

Until recently, most protein fluorescence work was carried out with 280-nm excitation. Nowadays, there is a trend toward employing 295-nm excitation to eliminate tyrosine fluorescence. As can be seen in Figure 6d, however, fluorescence from BSA is accompanied by a large Rayleigh scatter peak, which overlaps the BSA band sufficiently to preclude accurate measurement of either  $\Delta\lambda_{1/2}$  or the area under the BSA curve when 290-nm excitation is employed. The overlap is even greater with 295 or 300-nm excitation. Because of this Rayleigh scatter problem, we employed a lower excitation wavelength. 260-nm excitation was preferred to the frequently used 280-nm value, because the tryptophan/tyrosine molar absorbance ratio at 260 nm is about 50% larger than at 280 nm, so that the tyrosine contribution to the emission spectrum of BSA is significantly lower at the former wavelength.

### Dynamic and Static Quenching in Proteins Related to Location of Fluorophores

In native proteins only those fluorophores located at the hydrophilic surface should be dynamically quenched by solvent or by those surface quenching groups, e.g., hydrated carboxyl groups and carboxamide side chains<sup>23,24</sup> that are free to move in the vicinity of the fluorophores. On the other hand, since the relatively rigid environment in the hydrophobic interior should minimize the random motion of both the fluorophores and the quenching groups contained therein, e.g., ionized phenolic<sup>25</sup> and disulfide<sup>26</sup> groups, quenching in the interior should be mainly a static process. Using the classification of Burstein et al., static quenching would be expected for Class I tryptophan residues, and probably for Class II also, but Class III tryptophans should undergo dynamic quenching by solvent water.<sup>5</sup> (In our discussion we will adhere to Burstein's Class I-III notation only insofar as it relates to the location of a tryptophan residue, i.e., without regard to his  $\lambda_{\max}$  and  $\Delta\lambda_{1/2}$  assignments.) Dynamic quenching of a tryptophan-containing protein should, therefore, be indicated by a fluorescence lifetime, as well as a quantum yield, which is below that of unquenched free tryptophan, while for a protein that is only statically quenched the lifetime should be approximately equal to the unquenched free tryptophan value.

### Effect of Glycerol

We have previously shown<sup>5</sup> that the  $\tau$  value, 5.9 nsec, existent for a very dilute solution of tryptophan (0.01 mM) in glycerol closely approximates the  $\tau$  of unquenched tryptophan. The 5.7-nsec lifetime found for aqueous BSA, whose quantum yield ( $q' = 0.45$  for 260-nm excitation) is only about half of the quantum yield of tryptophan in glycerol, implies that the

quenching in aqueous BSA is primarily static. The fluorescent residues in aqueous BSA, therefore, cannot be in contact with mobile water, i.e., they are not Class III, since it is known<sup>5</sup> that H<sub>2</sub>O strongly quenches both tryptophan and tyrosine primarily by dynamic processes. Additional evidence for this conclusion is the complete insensitivity of the fluorescence lifetime and quantum yield (Figure 1a) of BSA to a fivefold increase in solvent viscosity, i.e., 1.1–5.5 cp, produced by addition of glycerol to an aqueous solution up to 50% v/v, whereas this solvent change increased both the quantum yield and the lifetime of free tryptophan about 40%.<sup>5</sup>

This lack of dependence on viscosity does not necessarily eliminate Class II as the proper designation for any fluorescent tryptophan in aqueous BSA, since it can be argued that the mean molecular diameter of glycerol,<sup>27</sup> 5.2 Å, prevents its penetration into small hydrophilic crevices in which Class II residues would be expected to reside. However, over the 0–50% glycerol range there is a blue shift of 6 nm in the  $\lambda_{\max}$  (Figure 1b) of the BSA fluorescence (260–290-nm excitation), which is twice as large as one observes for free tryptophan over the same solvent composition range. This difference suggests some increase in the hydrophobicity of the environment of the fluorophore, which probably is not attributable solely to increased glycerol concentration near a surface tryptophan. Such a change may be due to a small glycerol-induced conformational change, which causes movement of a nonpolar residue closer to the tryptophan. This would not necessarily affect the quantum yield and lifetime of the tryptophan, if the nonpolar residue does not participate in the quenching. These considerations could apply to Class II residues, or to Class I residues lying just below the surface of a crevice.

Indeed, a drastic conformation change definitely occurs in BSA when the solvent contains more glycerol than 50% v/v. This is evident from the sharp rise in the early part of the polarization curve shown in Figure 2, i.e., in the 50–70% glycerol range. For an ellipsoid of revolution of axial ratio  $<6$ , which includes BSA, the Perrin equation describing the polarization of the fluorescence simplifies<sup>28</sup> to

$$\left(\frac{1}{P} - \frac{1}{3}\right) = \left(\frac{1}{P_0} - \frac{1}{3}\right)(1 + KT\tau\eta^{-1}) \quad (5)$$

when the incident light is polarized.  $K$  equals  $(R/V)(\rho_0/\rho_h)$ , where  $R$  is the gas constant,  $V$  is the volume of the macromolecule,  $\rho_0$  is the rotatory relaxation time of a sphere of volume  $V$ , and  $\rho_h$  is the mean harmonic of the principal rotatory relaxation times of the ellipsoid.  $P_0$ , the limiting polarization in absence of rotation, is related to the angle  $\beta$  between emission and absorption oscillators by the Jablonski equation,<sup>29</sup>  $P_0 = (3 \cos^2 \beta - 1)/(3 + \cos^2 \beta)$ , when the incident light is polarized.

Since  $\rho_0/\rho_h$  is independent of viscosity,<sup>30</sup>  $KT$  should be constant for a given  $V$  and  $T$ . Hence, the abrupt (sevenfold) change in the slope of the  $P^{-1}$  versus  $\tau\eta^{-1}$  curve (Figure 2) at the 50% glycerol point must indicate a change in  $V$  and/or  $\beta$ . In this experiment there is no reason to expect a change in  $\beta$  without a change in  $V$ . It seems evident from Eq. (5) that

the direction of the slope change points to an increased macromolecular volume above the 50% glycerol point, such as would be produced by a sudden large swelling, or a suddenly accelerated swelling, of the macromolecule. Such a swelling could increase the distance between static-quenching groups and tryptophan residues, thereby tending to increase the quantum yield. However, at the same time, imbibition of solvent could continually accelerate as the conformational change proceeds, which could increase the motion of dynamic quenching groups and cause decreased quantum yield. The latter factor is demonstrated by the decreasing lifetime above the 50% glycerol point. The 10% increase in the quantum yield over the 50–70% glycerol range, however, shows that the decrease in static quenching outweighs the increased dynamic quenching. Both processes seem to continue above the 70% glycerol point, with the two quenching mechanisms becoming about equal in importance, i.e.,  $q'$  is constant while  $\tau$  continues to decrease. The fact that  $\tau$  continues to decrease all the way up to the 90% glycerol point despite the increasing solvent viscosity, suggests that the dynamic quenching groups are protein groups, made continually more mobile by the conformation change, rather than solvent water molecules. The continually decreasing  $\lambda_{\max}$  also attests to a continual change in the conformation.

The polarization data are not sufficiently accurate to allow their use to confirm any very small conformational change before the 50% glycerol point, such as was inferred above from the 6-nm change in  $\lambda_{\max}$ . Even though Figure 2 appears to be linear at the low-viscosity end, it must be noted that  $P$  varied only from 0.185 to 0.210. It would be useful to study the glycerol effect over this range with a fluorescent BSA conjugate having a much larger  $\tau/\rho_h$  ratio than nonconjugated BSA has, but in studies to date<sup>28,31</sup> with such conjugates  $T/\eta$  was varied by changing temperature rather than glycerol concentration.

### Effect of $\text{Cu}^{2+}$ Ions

From his finding that saturation of BSA with  $\text{Cu}^{2+}$  ions at pH 4.83 produces only 50% quenching, Luk<sup>32</sup> has concluded that one of the two tryptophans is unquenched by  $\text{Cu}^{2+}$  and is near the center of the macromolecule. That is, the unquenched tryptophan is too far from the surface to be influenced by the  $\text{Cu}^{2+}$ , which is known to bind only to the surface carboxyl groups at this pH.<sup>33</sup> Assuming Förster resonance transfer as the  $\text{Cu}^{2+}$  quenching mechanism, Luk calculated that the quenched residue must be within 14 Å of the macromolecular surface. From his observation that the fluorescence decay curve of aqueous BSA, measured by the single photon counting technique, appeared to be a single exponential, he concluded that the two tryptophan residues are in similar microenvironments. To support this conclusion one can also cite his finding that the  $\text{Cu}^{2+}$  quenching effect at pH 4.83 is not accompanied by any change either in the  $\lambda_{\max}$  or in the shape of the BSA emission spectrum.

These results, combined with our own glycerol-effect results, imply that either both tryptophan residues of BSA are Class II or that both are Class

I. Neither tryptophan should be accessible to water, since it is illogical to expect only 50% quenching by  $\text{Cu}^{2+}$  if both tryptophans are exposed to solvent water. Luk's results thus also contradict the model of Burstein et al. as it applies to BSA.

We have confirmed these observations of Luk for pH 5, but differ with his conclusion that the fluorescence lifetime is constant. Luk stated that his experimental error was 15%. We observed a decrease in  $\tau$  from 5.7 to 5.1 nsec with  $10^{-3} M \text{Cu}^{2+}$  at pH 5. We consider the reproducibility of our measurements to be better than 2% when  $\tau$  is 5–6 nsec, although the accuracy is probably 10–15%. It may be noted that our  $\tau$  measurement was made with 0.05% BSA, in which there is considerably less inner filter effect and light scattering than in the 0.5% BSA solution studied by Luk. Certainly, if  $\text{Cu}^{2+}$  quenches BSA fluorescence at pH 5 by Förster resonance transfer, as Luk assumed, one would expect a  $\text{Cu}^{2+}$  induced decrease in  $\tau$ .<sup>7</sup>

Henceforth in this paper, we will refer to the first quenched tryptophan, which we believe is in a hydrophobic microenvironment just below a crevice surface, as Try Ia, and will designate the second tryptophan, which we believe to be much closer to the macromolecular center, as Try Ib.

These conclusions are supported by the fact that  $\text{Cu}^{2+}$  quenches BSA fluorescence completely when a sufficiently strong conformation change is produced. This occurs with  $10^{-3} M \text{Cu}^{2+}$  at pH 7, where  $\text{Cu}^{2+}$  binds to imidazole and peptide groups, in addition to carboxyl groups.<sup>34</sup> Unlike at pH 5, the quenching (70%) caused by  $10^{-4} M \text{Cu}^{2+}$  at pH 7 is accompanied by a 7-nm blue shift in the emission  $\lambda_{\text{max}}$ , which cannot be attributed to any viscosity effect. The simultaneous lowering of  $\tau$  to 4.6 nsec, and to 4.2 nsec by  $2.5 \times 10^{-4} M \text{Cu}^{2+}$  (80% quenching), shows that this conformation change is drastic enough to produce dynamic quenching even of Try Ib.

Our evidence that both BSA tryptophan residues are below the macromolecular surface and that aqueous BSA is statically quenched suggests that the customary procedure of referencing the quantum yields of proteins to dynamically quenched aqueous tryptophan or tyrosine is misleading, even if, as Cowgill recommended,<sup>35</sup> the protein and the reference amino acid are measured under the same conditions of pH and temperature. It implies that there is some similarity in the quenching mechanism of the protein under study and the quenching mechanism of aqueous tryptophan or tyrosine, when, in fact, the close proximity of the quantum yields of aqueous BSA and aqueous tryptophan is fortuitous. The use of a quantity such as our  $q'$  parameter as a relative quantum yield for proteins seems preferable.

### Effects of Urea and Guanidine Hydrochloride

The initial effect on the fluorescence of BSA, when either urea or  $\text{GuHCl}$  is added to aqueous BSA, is shown by Figures 3 and 4 to be a reduction in the static quenching. This is demonstrated for each denaturant by the unchanging  $\tau$  up to a concentration of  $\sim 1 M$ , despite the 25% increase in  $q'$  to  $\sim 0.56$ . Any possibility that this initial increase in  $q'$  might be at-

tributable to onset of tyrosine fluorescence is eliminated by the initial constancy of  $\Delta\lambda_{1/2}$ . Further, there is no accompanying change in the polarization (Figure 5), so that no swelling of the macromolecule is evident at this point. Obviously, both of these denaturants have a significantly smaller effective diameter than glycerol has, so they can enter a hydrophilic crevice fairly easily. Then, either by reacting with surface protein groups directly, or indirectly by reacting with the crevice hydration layer, these denaturants can cause a small conformation change near Try Ia.

Some dynamic quenching becomes evident by the time the GuHCl concentrations [GuHCl] is raised to 1.6 *M*, where  $\tau$  has decreased to 4.8 nsec and  $q'$  has decreased back down to 0.47. With urea, however, dynamic quenching is not apparent until its concentration is 3 *M*. This implies that with 1.6 *M* GuHCl present the conformation change is enough to increase the *motion* of quenching groups near Try Ia and/or of Try Ia itself, while 2 *M* urea only causes *displacement* of the static-quenching group(s) and/or Try Ia. Consistent with this view is the increased  $\Delta\lambda_{1/2}$  in both cases, signifying the emergence of some tyrosine fluorescence, with the 5-nm enhancement produced by 1.6 *M* GuHCl being about twice that produced by 3 *M* urea.

The actual appearance of a tyrosine emission peak at 304 nm occurred by the time [GuHCl] reached 2.4 *M*. The relevant spectrum, along with the spectrum when [GuHCl] is 6.4 *M*, is shown in Figure 6. Simultaneously, as seen in Figure 3, 2.4 *M* GuHCl increased the half-width 24 nm, because of the tyrosine fluorescence, while  $q'$  and  $\tau$  both dropped sharply, to 0.3 and 3.1 nsec, respectively. The very drastic conformation change clearly demonstrated by these values is confirmed by the very large decrease in the polarization observed in the GuHCl curve of Figure 5 between the 1.6 *M* and 2.4 *M* points. The fact that, when [GuHCl] is 2.4 *M* or more,  $P$  lies considerably *below* the  $P$  value obtained with no denaturant present, despite the greatly decreased  $\tau$ , suggests that the conformation change increases the mobility of a tryptophan-containing portion of the macromolecule. That is, whereas  $P$  before the 2.4 *M* point is determined by the motion of the whole macromolecule, it reflects the motion of a tryptophan-containing segment after this point. Note that the change in  $P$  with GuHCl and urea is opposite to the direction of the glycerol-induced change, which we attributed above to a swelling of the macromolecule.

Denaturation at 15°C by GuHCl is not complete before 6.4 *M*, if then. This is evident from the continually increasing prominence of the tyrosine peak as [GuHCl] was raised up to 6.4 *M* (Figure 6), and by the decreasing  $\tau$  (3.0 to 2.5 nsec) and increasing  $q'$  (0.272 to 0.293) over the 4–6.4 *M* GuHCl range (Figure 3). This 7.4% increase in the  $q'$  value is barely significant (i.e., >5%), but it may indicate a decreasing rate of tyrosine-to-tryptophan energy transfer as the denaturation process increases the average distance between tyrosine and tryptophan residues. It also suggests that the fluorescence efficiency of the tyrosine residues when [GuHCl] > 4 *M* is slightly higher than the efficiency of fluorescence from those tryptophan residues that are excited by Förster energy transfer in the presence of 4 *M*, or more, GuHCl. There is no concomitant increase in  $\Delta\lambda_{1/2}$ , because the

maximum  $\Delta\lambda_{1/2}$ , i.e., the sum of the individual half-widths, 33 and 69 nm, is already attained by the time [GuHCl] reaches 3.2 *M*.

The identity of the tyrosine peak is evident from the fact that it appears at 304 nm upon excitation with 260- or 270-nm radiation, but does not appear with 290-nm excitation. This can be seen in Figure 6 despite the scatter peak interference. 280-nm excitation causes only an inflection near 304 nm. To our knowledge, this is the first report of an actual tyrosine peak being observed for a BSA solution, probably because of our use of ultra-pure denaturants. Our previous use of ordinary reagent grade denaturant did not produce a tyrosine peak. Cuatrecasas et al.<sup>36</sup> have observed it for staphylococcus nuclease in a 40% dioxane-H<sub>2</sub>O solvent mixture, while Kronman and Holmes<sup>37</sup> recorded a tyrosine shoulder for 6 *M* GuHCl-denatured rabbit muscle aldolase.

It can be seen in Figures 4 and 5 that the denaturation action of urea is much more gradual than the GuHCl action, as far as the denaturant concentration dependence is concerned. The following comparisons are of interest. 1) Tyrosine fluorescence was not directly observed until the urea concentration was 6 *M*, and even then it produced only a barely detectable shoulder near 312 nm, rather than a peak. This shoulder was quite visible with 7 and 8 *M* urea, and was at 304 nm at the latter point. 2) Urea did not cause *P* to plateau, but *P* decreased gradually over the 3–8 *M* urea range until at 8 *M* urea its value, 0.11, was only slightly above the plateau value, 0.10, produced by GuHCl above 2.4 *M*. 3)  $\tau$  decreased gradually over the 2–7 *M* urea range to a value, 3.1 nsec, which is a little higher than the  $\tau$  value, 2.5 nsec, observed when [GuHCl] was 6.4 *M*. 4) With urea solutions the half-width did not plateau, but it rose gradually to 99 nm for 8 *M* urea, only 2 nm smaller than the plateau value for 3.2–6.4 *M* GuHCl. 5)  $q'$  decreased gradually to approximately the same value, 0.28, with 6 *M* urea as was observed with GuHCl above 3 *M*. Thus, it appears that 8 *M* urea produces about as much denaturation of BSA as 3 *M* GuHCl does, which is definitely less than complete denaturation. Tanford<sup>38</sup> has reported a higher intrinsic viscosity for BSA in 6 *M* GuHCl (22.9 cm<sup>3</sup>/gm) than in 8 *M* urea (16.6 cm<sup>3</sup>/gm). From this and other results he has concluded that both urea and GuHCl produce random-coiled proteins, but that even a high urea concentration does not cause complete denaturation. Further, the optical rotatory dispersion studies of Tanford and his colleagues indicate that 6 *M* GuHCl completely denatures BSA, producing random coils.<sup>40</sup>

Our urea results are in agreement with the early work of Kauzmann and Simpson,<sup>39</sup> in that their curve for the urea dependence of the optical rotation of BSA at 20°C began between the 2 and 3 *M* urea points and it did not start to plateau even at the 8.5 *M* urea point. They made no observation with urea present at less than 2 *M*, however, so we are not certain whether the optical rotation technique can detect the change shown by the maximum at the 1 *M* urea point in our  $q'$  curve.

In a very recent paper,<sup>41</sup> Holmes and Robbins have claimed that their use of *N'*-methylnicotinamide chloride (NMNCl) as a quencher of protein fluorescence shows that one of the two BSA tryptophan residues is on the

surface. This, of course, is in conflict with our own conclusion that aqueous BSA contains no surface tryptophan. According to these authors the Stern-Volmer relationship holds for the quenching action of NMNCl with six of seven proteins studied, including BSA and HSA, although no BSA data were presented. From the fact that for three proteins in the native state and for five in 6 *M* GuHCl the Stern-Volmer constant  $K_q$  was considerably larger than the stability constant  $K_c$  for the charge-transfer complex that NMNCl forms with the tryptophan residues in these proteins, they concluded that NMNCl quenches protein fluorescence primarily by collisional action and is, therefore, a probe for surface tryptophan residues. No evidence for charge-transfer complexation of NMNCl by either BSA or HSA was obtained. The *assumption* was thus made that Stern-Volmer quenching, which cannot be attributed to static quenching, must be collisional. This is not a valid assumption, even though it is a widespread notion.

An alternative explanation for Stern-Volmer quenching of BSA fluorescence by NMNCl, which is in agreement with our contention that BSA contains no surface tryptophan, can be offered. Quenching would also obey Stern-Volmer kinetics if it were due primarily to very efficient Förster resonance transfer of excitation energy from the nonsurface Try Ia residue (i.e., just below the surface) to a nearby NMNCl molecule attached at the surface in a non-charge-transfer complex. In such a case, the mathematics would be similar to that of static quenching, which results from formation of a dark complex, and the Stern-Volmer constant would equal the stability constant of the complex.<sup>39</sup> Only fluorescence lifetime measurements, which Holmes and Robbins eschewed, can differentiate between collisional quenching and the "apparent" static quenching that we suggest for NMNCl quenching of BSA.<sup>42</sup> Their failure to detect a charge transfer complex does not also indicate absence of a non-charge-transfer complex, especially since the latter could be quite weak, i.e., a stability constant of 8.5 *M*<sup>-1</sup> corresponds to  $\Delta F^\circ = 1.3$  kcal/mol. The resonance transfer requirement that there be significant overlap between the fluorescence curve of BSA and the absorption curve of NMNCl<sup>43</sup> is met.

This paper is based on work performed under contract with the U.S. Atomic Energy Commission at the University of Rochester Atomic Energy Project, and has been assigned Report UR-49-577. It was partially supported by a Special Research Resource Grant PR-00220-07, from the Division of Research Resources of the National Institutes of Health, and the U.S. Public Health Service Training Grant 1T1 DE175.

## References

1. Teale, F. W. J. (1960) *Biochem. J.* **76**, 381-388.
2. Chen, R. F. (1967) in *Fluorescence, Theory, Instrumentation and Practice*, Guilbault, G. G., Ed., Marcel Dekker, New York, ch. 11, pp. 443-499.
3. Cowgill, R. W. (1969) in *Molecular Luminescence*, Lim, E. C., Ed., Benjamin, New York, pp. 589-605.
4. Burstein, E. A., Vedenkina, N. S. & Ivkova, N. M. (1973) *Photochem. Photobiol.* **18**, 263-279.



5. McGuire, R. & Feldman, I. (1973) *Photochem. Photobiol.* **18**, 119–124.
6. Weber, G. (1947) *Trans. Faraday Soc.* **44**, 185–189.
7. Forster, F. (1959) *Discuss. Faraday Soc.* **27**, 7–17.
8. Boaz, H. & Rollefson, G. K. (1959) *J. Amer. Chem. Soc.* **72**, 3435–3443.
9. Kauzmann, W. (1957) *Quantum Chemistry*, Academic, New York, p. 689.
10. Ettinger, R. H., Goldbaum, L. R. & Smith, Jr., L. H. (1952) *J. Biol. Chem.* **199**, 531–536.
11. Pitha, J. & Jones, R. N. (1966) *Can. J. Chem.* **44**, 3031–3050.
12. Azumi, T. & McGlynn, S. P. (1962) *J. Chem. Phys.* **37**, 2413–2420.
13. Perrin, F. (1929) *Ann. Phys. (Paris)* **12**, 169–275.
14. Weinryb, I. & Steiner, R. F. (1971) in *Excited States of Proteins and Nucleic Acids*, Steiner, R. F. & Weinryb, I. Eds., Plenum, New York, ch. 5, p. 288.
15. Longworth, J. W. (1971) in *Excited States of Proteins and Nucleic Acids*, Steiner, R. F. & Weinryb, I. Eds., Plenum Press, New York, ch. 6, p. 369.
16. Cowgill, R. W. (1969) *Fluoresc. News* **4**, 1–3.
17. Weber, G. (1960) *Biochem. J.* **75**, 345–352.
18. Sheely, M. L. (1932) *Ind. Eng. Chem.* **24**, 1060–1064.
19. Weber, G. (1961) *Biochem. J.* **79**, 29P–30P.
20. Weber, G. (1961) *Nature* **190**, 27–29.
21. Konev, S. V. (1967) in *Fluorescence and Phosphorescence of Proteins and Nucleic Acids*, Plenum, New York, p. 121.
22. Longworth, J. W. (1971) in *Excited States of Proteins and Nucleic Acids*, Steiner, R. F. & Weinryb, I. Eds., Plenum, New York, ch. 6, p. 431.
23. Cowgill, R. W. (1967) *Biochim. Biophys. Acta* **133**, 6–18.
24. Cowgill, R. W. (1970) *Biochim. Biophys. Acta* **200**, 18–25.
25. Edelhoch, H., Brand, L. & Wilchek, M. (1967) *Biochemistry* **6**, 547–572.
26. Cowgill, R. W. (1967) *Biochim. Biophys. Acta* **140**, 37–44.
27. Herskovits, T. T. & Sorenson, M. (1968) *Biochemistry* **7**, 2533–2541.
28. Steiner, R. F. & McAlister, A. J. (1957) *J. Polym. Sci.* **24**, 105–123.
29. Jablonski, A. (1935) *Z. Phys.* **96**, 236–246.
30. Tanford, C. (1963) in *Physical Chemistry of Macromolecules*, Wiley, New York, p. 359.
31. Weber, G. (1952) *Biochem. J.* **51**, 155–167.
32. Luk, C. K. (1971) *Biopolymers* **10**, 1229–1241.
33. Klotz, I. M. & Curme, H. G. (1948) *J. Amer. Chem. Soc.* **70**, 939–943.
34. Rao, M. S. N. & Lal, H. (1958) *J. Amer. Chem. Soc.* **80**, 3226–3235.
35. Cowgill, R. W. (1968) *Biochim. Biophys. Acta* **168**, 417–430.
36. Cuatrecasas, P., Edelhoch, H. & Anfinsen, C. B. (1967) *Proc. Nat. Acad. Sci., U.S.* **58**, 2043–2050.
37. Kronman, M. J. & Holmes, L. G. (1971) *Photochem. Photobiol.* **14**, 113–134.
38. Tanford, C. (1968) *Advan. Protein Chem.*, p. 174.
39. Kauzmann, W. & Simpson, R. B. (1953) *J. Amer. Chem. Soc.* **75**, 5154–5157.
40. Tanford, C., Kawahura, K., Lapanje, S., Hooker, Jr., T. M., Zarlengo, M. H., Salohuddin, A., Aune, K. C. & Takagi, T. (1967) *J. Amer. Chem. Soc.* **89**, 5023–5029.
41. Holmes, L. G. & Robbins, F. M. (1974) *Photochem. Photobiol.* **19**, 361–366.
42. Vaughan, W. M. & Weber, G. (1970) *Biochemistry* **9**, 464–473.
43. Guire, P. (1970) *Biochim. Biophys. Acta* **221**, 383–386.

Received July 29, 1974

Accepted October 23, 1974